MNX1 facilitates the malignant progress of lung adenocarcinoma through transcriptionally upregulating CCDC34

JUNHUA WU[1,2*], CHONGMEI YUE[1,2*], WEIGUO XU[1,2], HUI LI[1,2], JING ZHU[1,2] and LIN LI[1,2]

[1]Respiratory and Critical Care Medicine, Mianyang Central Hospital; [2]School of Medicine,
University of Electronic Science and Technology of China, Mianyang, Sichuan 621000, P.R. China

Abstract. Lung adenocarcinoma (LUAD) represents the most prevalent subtype of lung cancer and typically has high incidence and fatality rates. Motor neuron and pancreas homeobox 1 (MNX1) and coiled-coil domain-containing 34 (CCDC34) serve as oncogenes in multiple types of cancer. However, their role in LUAD remains to be elucidated. In the present study, bioinformatics analysis and LUAD cell lines were adopted to examine the expression of MNX1 and CCDC34. The proliferation, migration and invasion abilities of A549 cells were determined using Cell Counting Kit-8, colony formation, wound-healing and Transwell assay, and flow cytometry was conducted to assess cell cycle distribution and apoptosis. The interaction between MNX1 and CCDC34 was verified by luciferase reporter and chromatin immunoprecipitation assays. In addition, an *in vivo* animal model of LUAD was established for validation. The results demonstrated that both MNX1 and CCDC34 were upregulated in LUAD cell lines. MNX1 knockdown significantly suppressed cell proliferation, migration and invasion, hindered cell cycle progression and promoted cell apoptosis *in vitro* and inhibited tumor growth *in vivo*. However, the antitumor effect of MNX1 knockdown was weakened by simultaneous CCDC34 overexpression *in vitro*. In terms of mechanism, MNX1 was demonstrated to directly bind to the CCDC34 promoter and transcriptionally activate CCDC34 expression. In conclusion, the present study highlighted a critical role of the MNX1/CCDC34 axis in regulating LUAD progression, providing novel therapeutic targets for LUAD treatment.

Correspondence to: Dr Weiguo Xu, Respiratory and Critical Care Medicine, Mianyang Central Hospital, 12 Jingzhong Street, Fucheng, Mianyang, Sichuan 621000, P.R. China
E-mail: xwg522630@126.com

*Contributed equally

Introduction

Lung cancer represents a fatal malignancy accounting for the largest number of cancer-related deaths worldwide, accompanied by an estimated 2 million new cases and 1.8 million deaths annually (1,2). Lung adenocarcinoma (LUAD), a highly heterogeneous malignancy, is the most prevalent histological subtype of lung cancer occupying ~50% of reported cases (3,4). In recent years, despite the progress of multimodal treatment strategies, including surgical resection, chemoradiotherapy, molecular targeted therapy and emerging immunotherapies, the overall survival time of patients with lung cancer has not substantially improved (5). This has been mainly attributed to the deficiency of effective biomarkers for diagnosis and treatment. Hence, it is of urgent significance to identify more molecular mechanisms associated with LUAD development, so as to improve clinical diagnosis and treatment.

Motor neuron and pancreas homeobox 1 (MNX1), also termed HLXB9 or HB9, is located on chromosome 7q36.3 and is a homeodomain-containing transcriptional factor (6). MNX1 was initially discovered by Harrison *et al* (7) in pancreatic and lymphoid tissues, followed by the confirmation of the involvement of MNX1 in pancreatic and invertebrate development and motor neuronal differentiation (8-10). Subsequently, dysregulation of MNX1 was ascertained to be associated with Currarino syndrome, permanent neonatal diabetes in a consanguineous family and necrotizing enterocolitis of neonates (11-13). Emerging evidence has identified MNX1 as a novel oncogene that is upregulated in prostate, colorectal, cervical and breast cancer (14-17). However, the role of MNX1 in LUAD remains to be elucidated.

The coiled-coil domain (CCD), a structural motif identified and widely expressed in proteins, is associated with multiple biological functions, including gene expression regulation, membrane fusion, cell division and drug metabolism (18). Several reports have confirmed the connection between CCD-containing proteins (CCDC) and cancer. For example, CCDC43, CCDC137 and CCDC106 were distinctly upregulated in gastric cancer, hepatocellular carcinoma and lung cancer, respectively and have an association with the malignant phenotypes (19-21). CCDC34, also termed NY-REN-41, RAMA3 or L15, is located on chromosomes 11p14.1 and chromosome 11 is regarded as one of the most disease- and gene-rich chromosomes in the human

genome. CCDC34 was first discovered in hamartoma of the retinal pigment epithelium (22). Accumulating studies have illustrated the dysregulation of CCDC34 in hepatocellular carcinoma, colorectal cancer and bladder cancer, where it was associated with tumor cell growth, invasion and apoptosis (23-25). However, to the best of the authors' knowledge, whether CCDC34 is also involved in LUAD has yet to be reported.

Notably, it was predicted on the JASPAR website (https://jaspar.genereg.net/) that MNX1 may bind to the CCDC34 promoter, indicating a possible interaction between MNX1 and CCDC34. Based on this, the present study explored the role and function of MNX1 and CCDC34 in LUAD and further investigated their regulatory mechanism, proposing potential targets for the treatment of LUAD.

Materials and methods

Bioinformatic analysis. The Gene Expression Profiling Interactive Analysis (GEPIA, http://gepia.cancer-pku.cn/) cancer database was mined to assess the expression level of MNX1 and CCDC34 in LUAD tumor (n=483) and normal tissues (n=347). Meanwhile, the overall survival curves of patients with LUAD were plotted using the Kaplan-Meier method with log-rank test.

Cell culture. Human bronchial epithelial cells, BEAS-2B (cat. no. BNCC359274) and the human LUAD cells, PC-9 (cat. no. BNCC340767), were purchased from BeNa Culture Collection. Human LUAD cell lines, A549 (cat. no. CL-0016) and H1975 (cat. no. CL-0298), were provided by Procell Life Science & Technology Co. Ltd. and the H3255 cell line (cat. no. Bio-106227) was provided by Biobw Biotechnology Co., Ltd. All cell lines were maintained in Dulbecco's Modified Eagle's medium (Gibco; Thermo Fisher Scientific, Inc.) with 10% fetal bovine serum (FBS; Gibco; Thermo Fisher Scientific, Inc.) at 37°C in a humidified atmosphere incubator with 5% CO_2.

Reverse transcription-quantitative (RT-q) PCR. Total RNA was extracted from A549 cells using TRIzol® reagent (Thermo Fisher Scientific, Inc.) according to the manufacturer's instructions and quantified. A total of 1 µg of RNA was reverse transcribed into cDNA using M-MLV Reverse Transcriptase (Promega Corporation) according to the manufacturer's protocol. The qPCR procedure was conducted utilizing SYBR-Green (Takara Bio, Inc.) on a ABI7500 quantitative PCR instrument (Thermo Fisher Scientific, Inc.) in line with the manufacturer's guidelines. The thermocycling conditions were as follows: 94°C for 5 min, followed by 40 cycles at 94°C for 15 sec, 60°C for 25 sec and 72°C for 30 sec. The sequences of primers used were as followed: MNX1, forward, 5'-GCC TAAGATGCCCGACTTCAAC-3', reverse, 5'-CGCGACAGG TACTTGTTGAGCT-3'; CCDC34, forward, 5'-ACAGAAACA GGTGCGCTTACC-3', reverse, 5'-CAGCCGGTCACGTTC TTCTTT-3'; β-actin, forward, 5'-AGCGAGCATCCCCCA AAGTT-3', reverse, 5'-GGGCACGAAGGCTCATCATT-3'. Gene expression was calculated by $2^{-\Delta\Delta Cq}$ (26) and normalized to the housekeeping gene β-actin. All experiments were repeated three times.

Western blotting. Total protein was extracted using radioimmunoprecipitation assay (Beyotime Institute of Biotechnology) and protein concentration was quantified using the bicinchoninic acid method (Beyotime Institute of Biotechnology). Subsequently, the denatured proteins (30 µg/lane) were resolved on 12% SDS-PAGE gels and transferred onto PVDF membranes (MilliporeSigma). After being blocked with 5% skimmed milk at room temperature for 2 h, the membranes were probed overnight with primary antibodies against MNX1 (dilution 1:1,000; cat. no. 41983; Cell Signaling Technology, Inc.), Ki67 (dilution 1:1,000; cat. no. ab16667; Abcam), proliferating cell nuclear antigen (PCNA; dilution 1:3,000; cat. no. ab29; Abcam), LaminB1 (dilution 1:10,000; cat. no. ab16048; Abcam), MMP2 (dilution 1:1,000; cat. no. 10373-2-AP; Proteintech Group, Inc.), MMP9 (dilution 1:1,000; cat. no. 10375-1-AP; Proteintech Group, Inc.), Cyclin B1 (dilution 1:50,000; cat. no. ab32053; Abcam), p-Histone H2A.X (dilution 1:1,000; cat. no. 9718; Cell Signaling Technology, Inc.), Bcl-2 (dilution 1:1,000; cat. no. ab196495; Abcam), Bax (dilution 1:1,000; cat. no. ab32503; Abcam), cleaved-caspase3 (dilution 1:1,000; cat. no. 9661; Cell Signaling Technology, Inc.), cleaved-caspase9 (dilution 1:1,000; cat. no. 7237; Cell Signaling Technology, Inc.), CCDC34 (dilution 1:1,000; cat. no. ab122396; Abcam) and GAPDH (dilution 1:2,500; cat. no. ab9485; Abcam) at 4°C overnight, followed by incubation with goat anti-rabbit (dilution 1:3,000; cat. no. ab6721; Abcam) or goat anti-mouse (dilution 1:2,000; cat. no. Ab6789; Abcam) secondary antibodies conjugated to horseradish peroxidase for 2 h at room temperature. The target bands were examined using a Bio-Rad gel imaging system (Bio-Rad Laboratories) with an ECL reagent (MilliporeSigma). Finally, the blots were semi-quantified with ImageJ software (version 1.52; National Institutes of Health).

Cell transfection. Short hairpin (sh) RNA (pGPU6 plasmid) targeting MNX1 (sh-MNX1-1, forward, 5'-CCGGGCAGG AAGCGGAGAAACAGAACTCGAGTTCTGTTTCTC CGCTTCCTGCTTTTTG-3' and reverse, 5'-AATTCAAAA AGCAGGAAGCGGAGAAACAGAACTCGAGTTCTGTTT CTCCGCTTCCTGC-3'; sh-MNX1-2, forward, 5'-CCGGCG AGGACGACGAGGACCATTTCTCGAGAAATGGTC CTCGTCGTCCTCGTTTTTG-3' and reverse, 5'-AATTCA AAAACGAGGACGACGAGGACCATTTCTCGAGAAATG GTCCTCGTCGTCCTCG-3'), pcDNA3.1 vector expressing MNX1 (oe-MNX1) or CCDC34 (oe-CCDC34) and the negative control (NC) of shRNA (sh-NC, 5'-CCGGCAACAAGA TGAAGAGCACCAACTCGAGTTGGTGCTCTTCATCTT GTTGTTTTTG-3') and pcDNA3.1 (oe-NC) were obtained from Shanghai GenePharma Co., Ltd. A549 cells (1x10⁵) were aliquoted into 6-well plates. Upon achieving 60-70% confluency, cells were transfected with sh-MNX1-1/2 (50 nM), sh-NC (50 nM), oe-MNX1 (40 nM), oe-CCDC34 (40 nM) or oe-NC (40 nM) plasmids using Lipofectamine® 3000 (Invitrogen; Thermo Fisher Scientific, Inc.) at 37°C for 48 h in accordance with the manufacturer's protocol. Thereafter, the cells were harvested for detecting transfection efficacy using RT-qPCR and western blotting.

Cell proliferation assays. Cell proliferation ability was assessed using Cell Counting Kit-8 (CCK-8) and colony

formation assays. For the CCK-8 assay, A549 cells were aliquoted into 96-well plates (1×10^4 cells/well). After incubation at 37°C and 5% CO_2 for 24, 48 and 72 h, 10 μl of CCK-8 solution (Nanjing KeyGen Biotech Co., Ltd.) was added to each well for a further 2 h incubation. The absorbance at 450 nm was measured using a spectrophotometer (Synergy H1; Omega Bio-Tek, Inc.). For the colony formation assay, A549 cells were aliquoted in 6-well plates (1×10^3 cells/well). Following incubation for 2 weeks, 4% paraformaldehyde was utilized to fix the colonies for 15 min at room temperature, followed by staining with 1% crystal violet for 20 min at room temperature. The colonies (>50 cells) were observed and counted using ImageJ software (version 1.52; National Institutes of Health).

Cell migration assay. A549 cells (5×10^4) were aliquoted into 96-well plates for culturing until cell confluency achieved 100%. A straight wound was generated using a 200 μl pipette tip. The plates were washed with PBS to wipe out the deciduous cells and serum-free medium was applied for the further incubation for 48 h at 37°C. Images of the wounds were captured at 0 and 48 h under a light microscope (Nikon Corporation).

Cell invasion assay. A 24-well plate containing 8-μm pore inserts precoated with Matrigel (Corning, Inc.) for 30 min at 37°C was used for the cell invasion assay. A549 cells (5×10^4) were aliquoted into the upper chamber and allowed to invade towards the lower chamber, which contained the complete medium supplemented with 10% FBS. Following incubation at 37°C for 48 h, the invaded cells were fixed with 4% paraformaldehyde for 15 min at room temperature, stained with 1% crystal violet for 20 min at room temperature and were finally observed under a light microscope (Nikon Corporation).

Flow cytometry assay. Cell cycle and apoptosis were evaluated via flow cytometry analysis. For the cell cycle assay, A549 cells were washed with PBS and fixed in 70% ethanol at 4°C for 1 h. Subsequently, cells were stained with 2 mg/ml propidium iodide (40X; MilliporeSigma) supplemented with 10 mg/ml RNase (100X; Thermo Fisher Scientific, Inc.) at room temperature for 30 min away from light, followed by detection with a FACS C6 flow cytometer (Becton, Dickinson and Company) and analysis with FlowJo v7.6 software (FlowJo LLC). For the cell apoptosis assay, cells were washed with pre-cooled PBS and then resuspended in binding buffer (1X), followed by staining with propidium iodide and Annexin V, according to the instructions of an Annexin V-FITC apoptosis kit (Dalian Meilun Biology Technology Co., Ltd.). Finally, the cell apoptotic rate (the percentage of early + late apoptotic cells) was examined using the aforementioned flow cytometer.

Luciferase reporter assay. The wild-type (WT) and mutant (MUT) sequences of the CCDC34 promoter were inserted into pGL3 luciferase reporter vectors (Promega Corporation) to construct CCDC34-WT and CCDC34-MUT vectors. A549 cells (1×10^5) were aliquoted into 6-well plates and incubated at 37°C overnight. Cells were transfected with oe-NC or oe-MNX1 and co-transfected with CCDC34-WT or CCDC34-MUT vectors using Lipofectamine® 3000 (Invitrogen; Thermo Fisher Scientific, Inc.), according to the manufacturer's protocol. After 48 h of transfection, the luciferase activity was detected using a dual-luciferase reporter system (Promega Corporation) and normalized to *Renilla* luciferase activity.

Chromatin immunoprecipitation (ChIP) assay. A549 cells (2×10^6 cells/assay) were cross-linked with 1% formaldehyde for 10 min at 37°C and quenched with glycine, followed by washing with ice-cold PBS, and cell lysis with SDS lysis buffer (Upstate Biotechnology, Inc.). The lysates were sonicated (20 kHz) into chromatin fragments with a 10-sec on and 10-sec off mode for 12 cycles on ice. Subsequently, 2% of the supernatant served as the input, and the remaining 100 μl of the supernatants were cultured overnight with 60 μl A/G agarose beads (Cell Signaling Technology, Inc.) at 4°C, followed by incubation with anti-MNX1 antibody (dilution 1:50; cat. no. 41983; Cell Signaling Technology, Inc.) or the negative control IgG (dilution 1:50; cat. no. 2729; Cell Signaling Technology, Inc.) at 4°C overnight. The precipitated DNA was purified and then detected by RT-qPCR as aforementioned.

Animal experiments. A total of 12 BALB/c nude male mice (4-5 weeks old; weight, 18-22 g) were provided by Shanghai SLAC Laboratory Animal Co., Ltd. and housed under specific pathogen-free conditions at 23-25°C, controlled humidity of 50-70%, under a 12-h light/dark cycle, and with free access to food and water. After acclimation for 1 week, all mice were randomly assigned into two groups (n=6 per group): i) sh-NC group; A549 cells (2×10^6 cells) infected with lentivirus containing sh-NC were subcutaneously injected into the left flank of mice; and ii) sh-MNX1 group; A549 cells (2×10^6 cells) infected with lentivirus containing sh-MNX1 were subcutaneously injected into the left flank of mice. Animal body weight and tumor size were monitored every 3 days and the tumor volumes were calculated using the formula: (length x width^2)/2. After continuous feeding for 21 days (the longest length of the tumor did not exceed 1.5 cm at this time point), all mice were sacrificed by administering an intraperitoneal injection of pentobarbital sodium (50 mg/kg body weight) and rapid cervical dislocation. Tumors were extracted for weighing and were stored at -80°C for western blot analysis. All animal experiments were implemented in accordance with the guidelines and protocols for animal care and were approved by the Ethics Committee of Mianyang Central Hospital [approval no. S2021097 (01)].

Statistical analysis. The results analyzed by GraphPad Prism version 8.0 (Dotmatics) were presented as mean ± SD. Comparison analysis was implemented using Student's unpaired t-test between two groups and using one-way ANOVA analysis with Tukey's post hoc test among more than two groups. $P<0.05$ was considered to indicate a statistically significant difference.

Results

MNX1 is upregulated in LUAD. First, it was evident from the analysis of datasets from the GEPIA database that the MNX1 expression level in LUAD tumor tissues was significantly higher than that in normal tissues (Fig. 1A). Meanwhile, patients with LUAD with a high level of MNX1 were associated
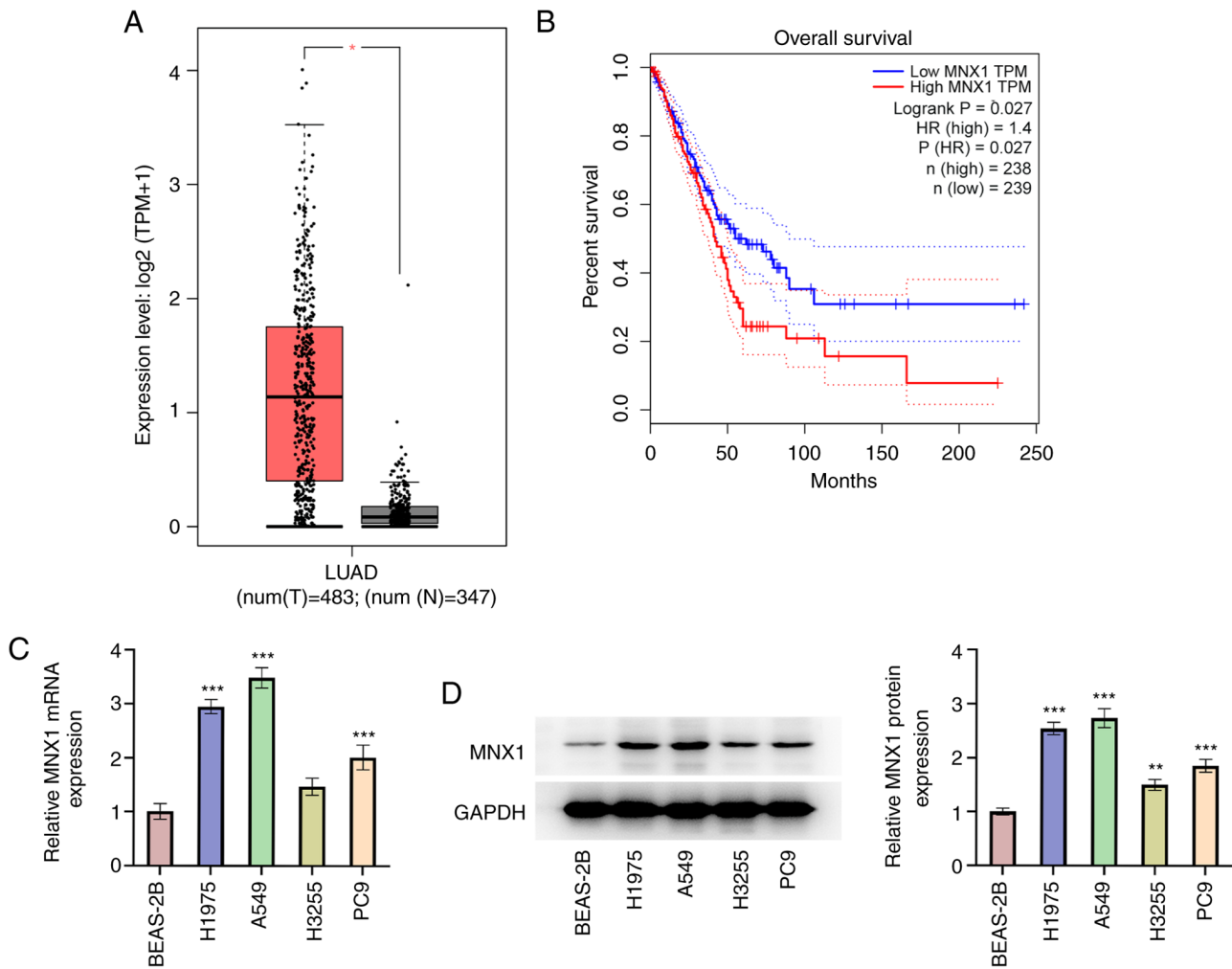
Figure 1. MNX1 is upregulated in LUAD. GEPIA database exhibited (A) the MNX1 expression level in tumor tissues of LUAD and (B) the overall survival of LUAD patients with high or low expression of MNX1. Human bronchial epithelial cells BEAS-2B and human LUAD cell lines (PC-9, A549, H1975 and H3255) were used to examine the (C) mRNA level and (D) protein expression of MNX1 using reverse transcription-quantitative PCR and western blotting, respectively. *P<0.05, **P<0.01, ***P<0.001 vs. BEAS-2B. MNX1, Motor neuron and pancreas homeobox 1; LUAD, Lung adenocarcinoma; GEPIA, Gene Expression Profiling Interactive Analysis.

with a poor overall survival (Fig. 1B). Next, the expression level of MNX1 in human bronchial epithelial cells (BEAS-2B) and human LUAD cell lines (PC-9, A549, H1975 and H3255) was examined. It is shown in Fig. 1C and D that LUAD cell lines, especially the A549 cell line, possessed a relatively high level of MNX1 compared with the BEAS-2B cell line, further confirming the aberrant upregulation of MNX1 in LUAD.

MNX1 knockdown represses proliferation, migration and invasion of A549 cells. To clarify the specific role of MNX1 in LUAD, cell transfection with MNX1 shRNA was implemented in A549 cells. Following transfection with sh-MNX1-1 or sh-MNX1-2, both the mRNA and protein expression levels of MNX1 were notably downregulated (Fig. 2A and B). Due to a higher transfection efficacy, sh-MNX1-1 was selected for subsequent experiments. Compared with the sh-NC group, sh-MNX1 not only repressed the proliferation ability of A549 cells, evidenced by the decreased cell viability and number of colonies, but also diminished the migration and invasion abilities of A549 cells (Fig. 2C-G). In addition, a marked decrease in the level of proliferation-related proteins (Ki67 and PCNA)

and invasion-related proteins (MMP2 and MMP9) in the sh-MNX1 group (Fig. 2H) was observed, further confirming the antiproliferative and anti-invasive properties of the MNX1 knockdown.

MNX1 knockdown hinders cell cycle progression and promotes apoptosis of A549 cells. In addition, according to flow cytometry analysis, it was observed that the proportion of cells in S phase was decreased in the sh-MNX1 group compared with the sh-NC group, while cell cycle arrest in G_2/M was increased, suggesting that MNX1 knockdown may hinder cell cycle progression (Fig. 3A). Cyclin B1 accumulates steadily during G_2 phase to promote G_2/M transition. Phosphorylated (p)-histone H2A.X is a DNA double strand break marker related to checkpoint signaling (27). In the present study, it was observed that MNX1 knockdown lowered the protein levels of cyclin B1 and p-histone H2A.X (Fig. 3B). This further demonstrated that MNX1 knockdown resulted in a delay in transition at G_2/M phase, thereby stalling cell cycle progression. Furthermore, a prominent elevation of cell apoptosis rate was observed in the sh-MNX1 group,
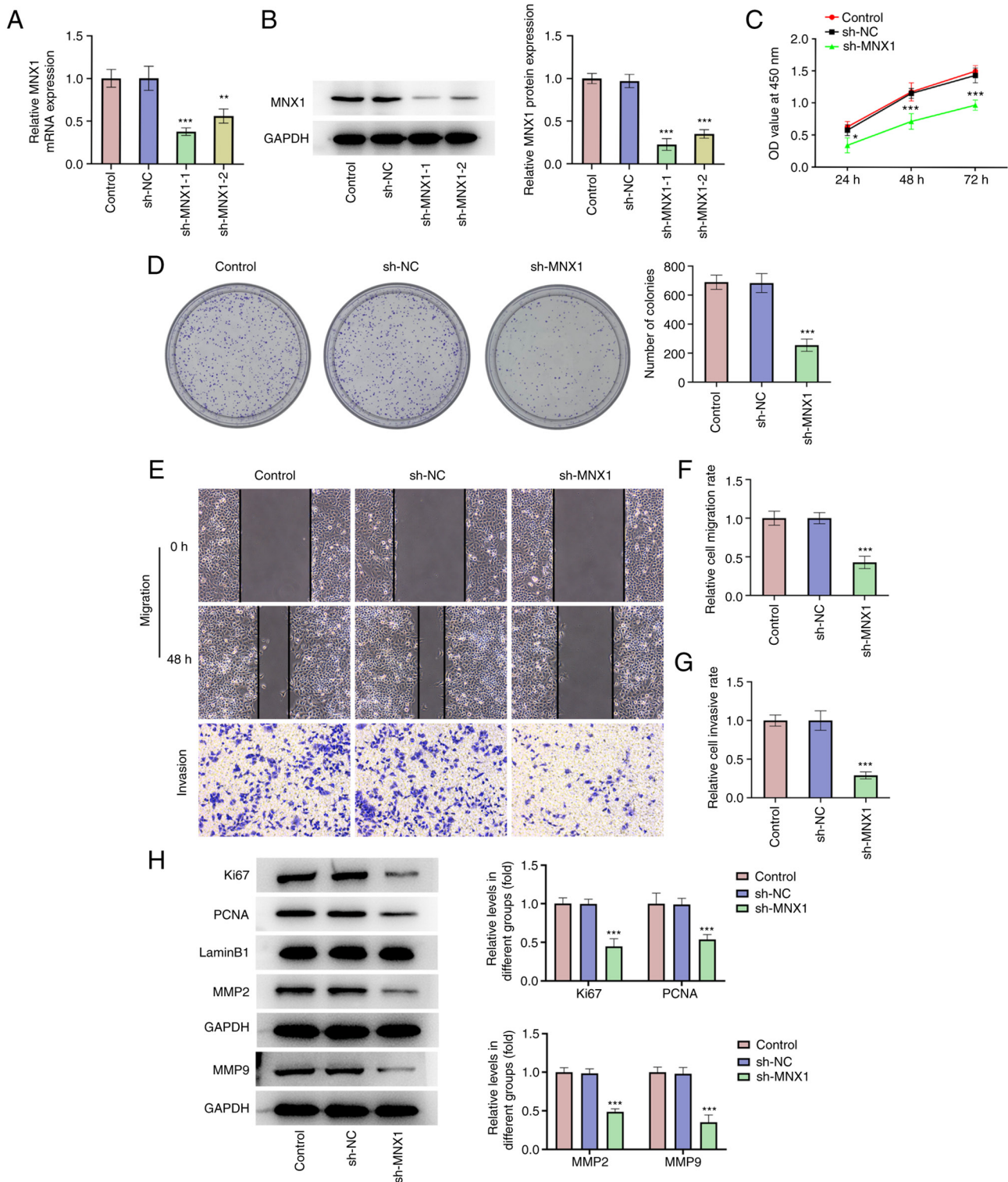
Figure 2. MNX1 knockdown represses proliferation, migration and invasion of A549 cells. Following transfection with sh-NC or sh-MNX1-1/sh-MNX1-2 in A549 cells, (A) the mRNA level and (B) protein expression of MNX1 were examined using reverse transcription-quantitative PCR and western blotting, respectively. (C) CCK-8 assay was used to examine cell viability. (D) Cell colony formation assay was conducted to assay formed colonies. (E-G) Wound-healing and Transwell assays were performed to examine cell migration and invasion, respectively. Magnification, x100. (H) Protein expression of Ki67, PCNA, MMP2 and MMP9 was examined using western blotting. *P<0.05, **P<0.01, ***P<0.001 vs. sh-NC. MNX1, Motor neuron and pancreas homeobox 1; sh, short hairpin RNA; NC, negative control (empty vector); CCK-8, Cell Counting Kit-8; PCNA, proliferating cell nuclear antigen.

accompanied with downregulation of Bcl-2 and upregulation of Bax, cleaved-caspase3 and cleaved-caspase9 (Fig. 3C and D), suggesting that MNX1 knockdown also facilitated cell apoptosis of A549 cells.

MNX1 knockdown inhibits tumor growth in vivo. To verify the antitumor activity of MNX1 in LUAD, an *in vivo* animal model was established. The daily monitoring of the animals in the study demonstrated that the body weight of the mice in
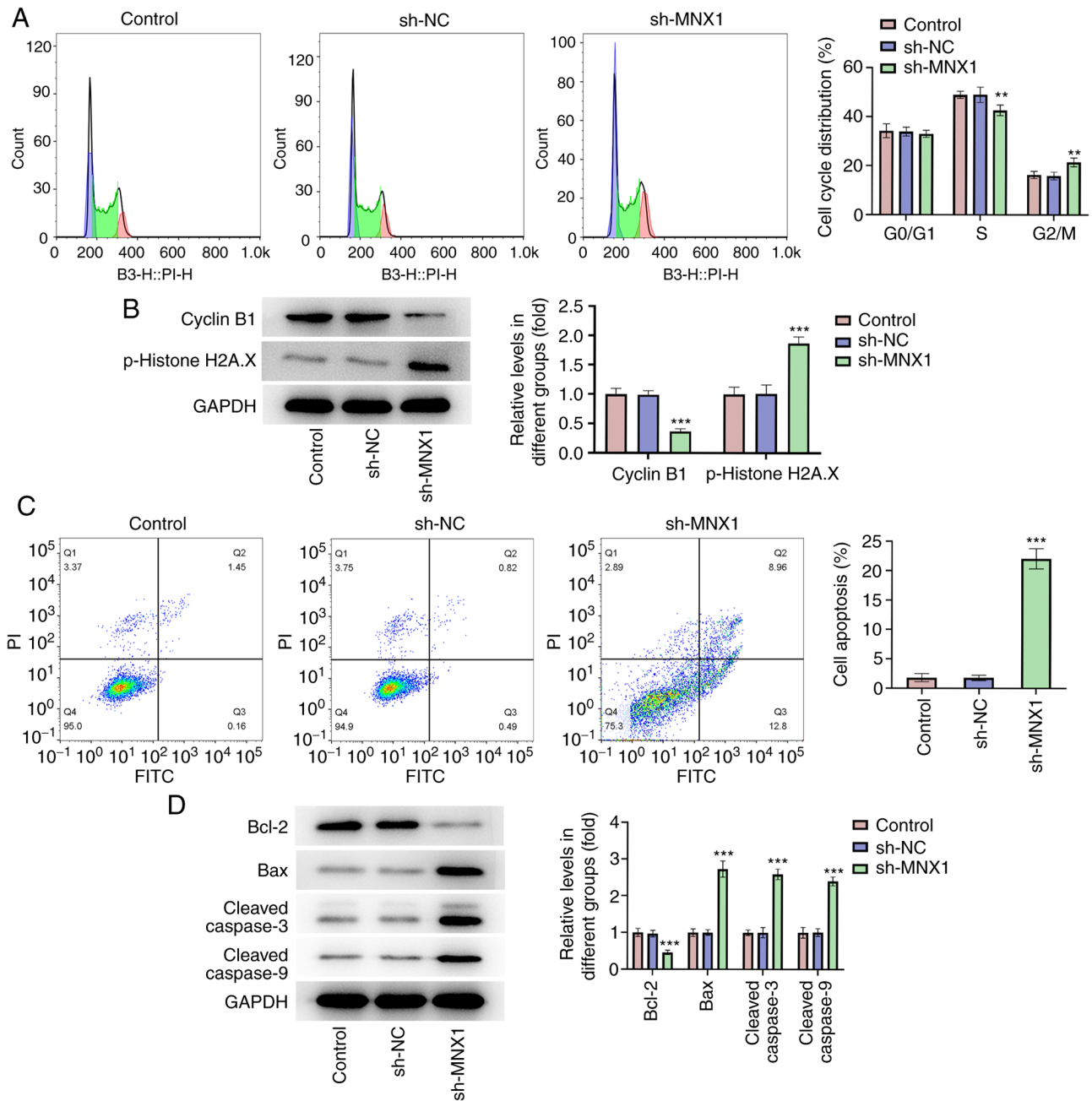
Figure 3. MNX1 knockdown hinders cell cycle progression and promotes apoptosis of A549 cells. Following transfection with sh-NC or sh-MNX1 in A549 cells, (A) Cell cycle distribution was assessed using flow cytometry analysis. (B) Protein expression of cyclin B1 and p-Histone H2A.X was detected using western blotting. (C) Cell apoptosis rate was detected using flow cytometry analysis. (D) Protein expression of Bcl-2, Bax, cleaved-caspase3 and cleaved-caspase9 was detected using western blotting. $^{**}P<0.01$, $^{***}P<0.001$ vs. sh-NC. MNX1, Motor neuron and pancreas homeobox 1; sh, short hairpin RNA; NC, negative control (empty vector); p-, phosphorylated.

the sh-NC and sh-MNX1 groups increased steadily, without a significant difference between the two groups (Fig. 4A). However, the tumor volume in the sh-MNX1 group was markedly smaller than that in the sh-NC group (Fig. 4B). After sacrificing the mice, the tumors were extracted and examined and a smaller tumor size and a lower tumor weight were observed in the sh-MNX1 group (Fig. 4C and D). Meanwhile, the protein expression level of Ki67 and PCNA in tumor tissues was markedly decreased in the sh-MNX1 group (Fig. 4E).

MNX1 binds to the CCDC34 promoter and transcriptionally regulates CCDC34 expression. Next, the expression profile of

CCDC34 in LUAD was examined. As assessed by the GEPIA database, CCDC34 was highly expressed in LUAD tumor tissues (Fig. 5A), which was consistent with the following results where the expression level of CCDC34 in A549 cells was higher than that in BEAS-2B cells (Fig. 5B and C). Subsequently, to understand the connection between MNX1 and CCDC34, a successful transfection of a MNX1 overexpression vector was first verified (Fig. 5D and E). The expression level of CCDC34 was subsequently demonstrated to be upregulated following MNX1 overexpression, whereas it was downregulated following MNX1 knockdown (Fig. 5F and G). These results demonstrated that MNX1
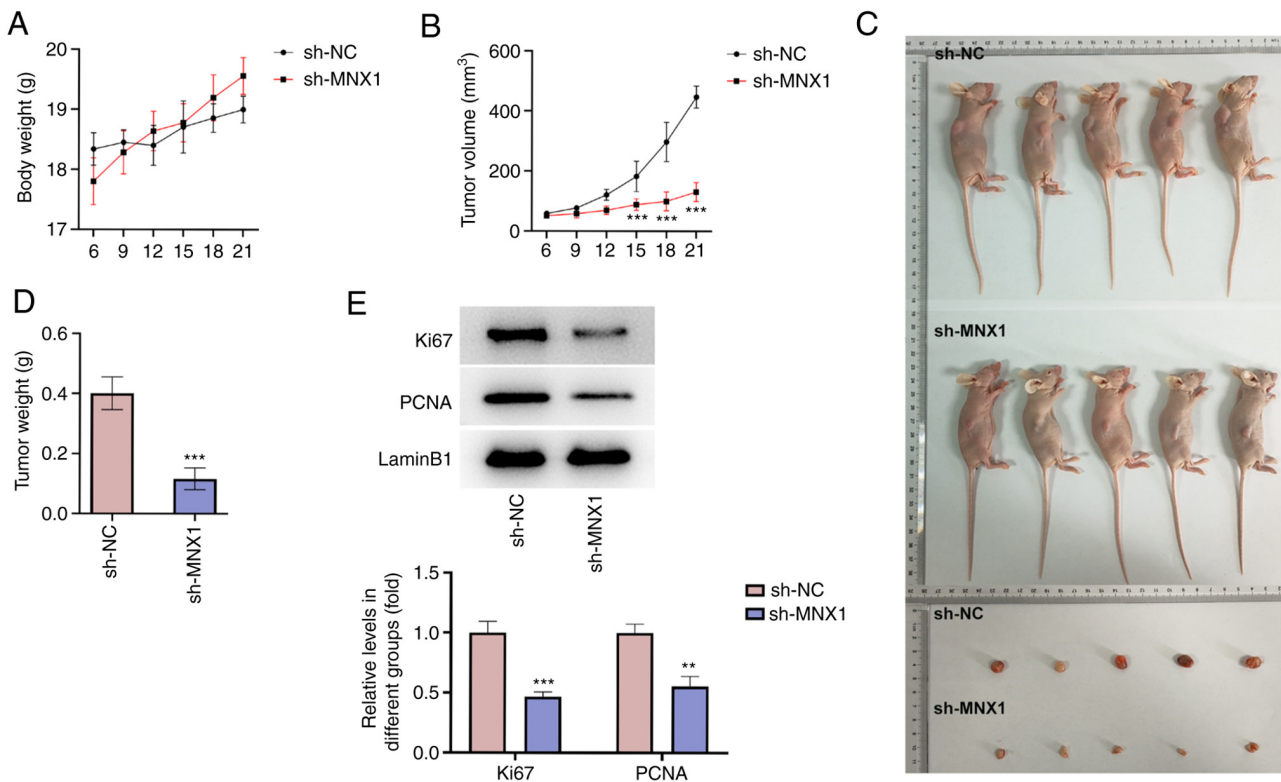
Figure 4. MNX1 knockdown inhibits tumor growth *in vivo*. An *in vivo* LUAD animal model was established and the (A) body weight and (B) tumor volume were monitored every 3 days. (C) After sacrifice, the tumors were taken out and images captured. (D) Tumor weight was recorded. (E) Protein expression of Ki67 and PCNA in tumor tissues was detected using western blotting. **P<0.01, ***P<0.001 vs. sh-NC. MNX1, Motor neuron and pancreas homeobox 1; LUAD, Lung adenocarcinoma; sh, short hairpin RNA; NC, negative control (empty vector); PCNA, proliferating cell nuclear antigen.

may regulate CCDC34 expression in A549 cells. Moreover, based on the prediction from the JASPAR website, MNX1 may bind to the CCDC34 promoter (Fig. 5H). This prediction was verified by luciferase reporter assay and ChIP assay where MNX1 overexpression significantly increased the luciferase activity of in CCDC34-WT group and CCDC34 was enriched in anti-MNX1 group compared to the anti-IgG group (Fig. 5I and J).

CCDC34 overexpression abolishes the inhibitory effect of MNX1 knockdown on the malignant phenotypes of A549 cells. To further establish the regulatory role of MNX1/CCDC34 in LUAD, the successful transfection of a CCDC34 overexpression vector was first verified (Fig. 6A and B). Then, A549 cells were transfected with sh-MNX1 alone or co-transfected with oe-NC/oe-CCDC34. A series of *in vitro* assays including CCK-8, colony formation, wound-healing and Transwell assays revealed that the inhibitory effects of MNX1 knockdown on cell proliferation, migration and invasion abilities in A549 cells were partly abolished by CCDC34 overexpression (Fig. 6C-G), which was also verified by the restored protein expression of Ki67, PCNA, MMP2 and MMP9 in the sh-MNX1 + oe-CCDC34 group compared with the sh-MNX1 + oe-NC group (Fig. 6H). Additionally, CCDC34 overexpression may facilitate cell cycle progression, which was hindered by MNX1 knockdown, through diminishing cell cycle arrest in G_2/M phase, accompanied by the restored protein levels of cyclin B1 and p-histone H2A.X (Fig. 7A and B). Meanwhile, the elevated apoptosis rate induced by MNX1 knockdown

was also diminished by CCDC34 overexpression, as well as the upregulation of Bcl-2 and downregulation of Bax, cleaved-caspase3 and cleaved-caspase9 (Fig. 7C and D).

Discussion

LUAD, representing the most prevalent subtype of lung cancer, typically has high incidence and fatality rates (28). Despite improvements in LUAD therapeutic strategies, the outcomes remain suboptimal and the 5-year overall survival rate is <20% (29). Identification of reliable diagnostic or prognostic biomarkers is beneficial to the development of specific therapeutic targets in the field of cancer gene therapy, to improve the overall survival of patients (30).

MNX1 exerts an oncogenic role in multiple types of cancer such as colorectal cancer and cervical cancer and the epigenetic silencing of which suppresses proliferation, migration and invasion of cancer cells *in vitro* and restricted tumor growth *in vivo*, while MNX1 overexpression may accelerate tumorigenicity (15,16,31). However, studies supporting the oncogenic role of MNX1 in LUAD are few. In the present study, using bioinformatic analysis and the clinicopathological data of LUAD, it was revealed for the first time, to the best of the authors' knowledge, that patients with LUAD had a relatively high level of MNX1 and a patient with a high level of MNX1 was associated with a poor survival outcome. Consistently, the subsequent *in vitro* and *in vivo* assays confirmed that MNX1 knockdown hindered the malignant phenotypes of LUAD cells, such as proliferation, migration and invasion and restricted
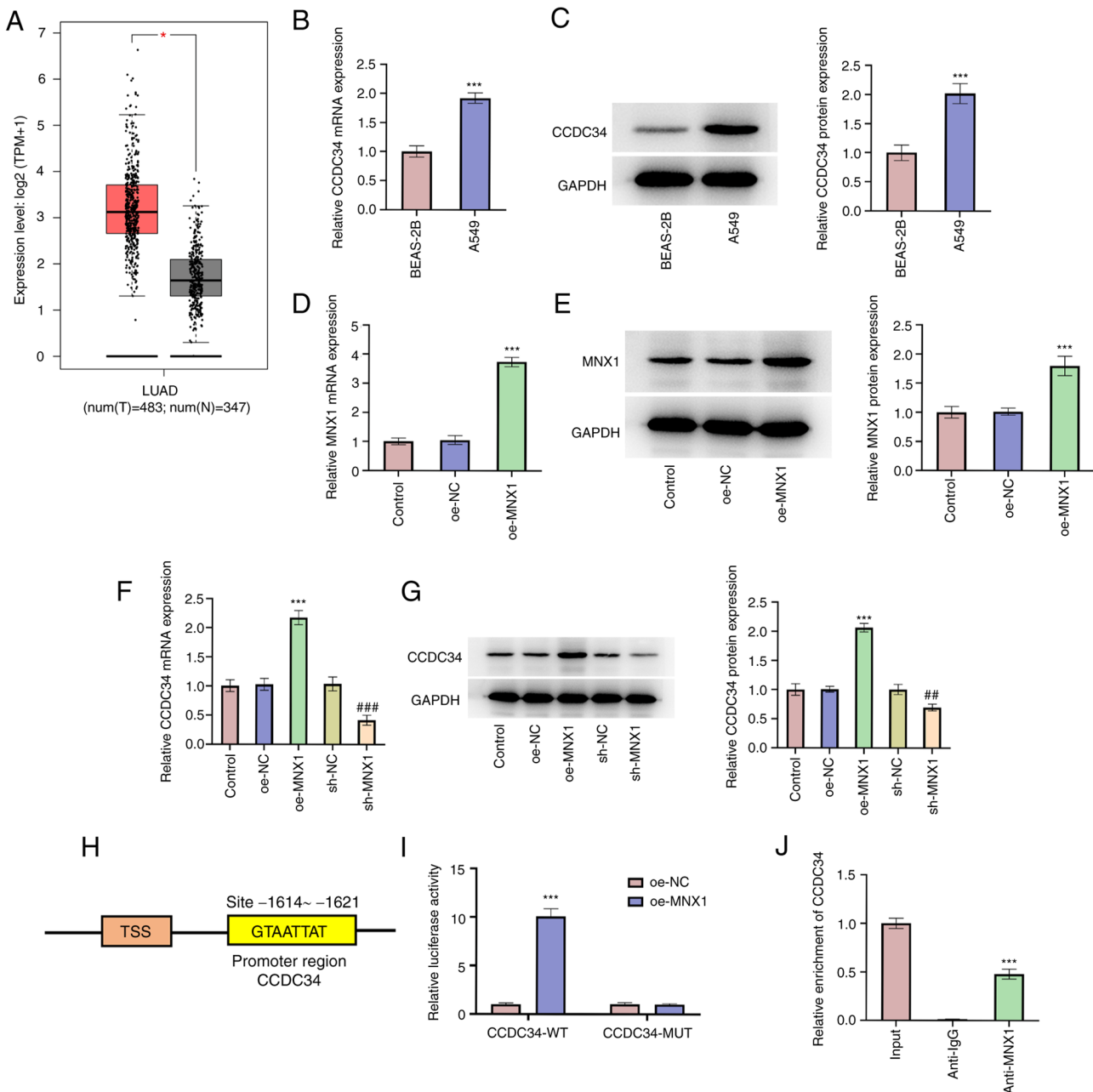
Figure 5. MNX1 binds to CCDC34 promoter and transcriptionally regulates CCDC34 expression. (A) GEPIA database exhibited the CCDC34 expression level in tumor tissues of LUAD. *P<0.05. Human bronchial epithelial cells BEAS-2B and human LUAD cell lines A549 were applied to examine the (B) mRNA level and (C) protein expression of CCDC34 using RT-qPCR and western blotting, respectively. ***P<0.001 vs. BEAS-2B. A549 cells were transfected with oe-NC or oe-MNX1 and the (D) mRNA level and (E) protein expression of MNX1 using reverse RT-qPCR and western blotting, respectively. A549 cells were transfected with oe-MNX1 or sh-MNX1 or their negative controls and the (F) mRNA level and (G) protein expression of CCDC34 using RT-qPCR and western blotting, respectively. ***P<0.001 vs. oe-NC; $^{##}$P<0.01, $^{###}$P<0.001 vs. sh-NC. (H) As predicted from JASPAR website, MNX1 might bind to CCDC34 promoter. (I) Luciferase reporter assay was performed to verify the interaction between MNX1 and CCDC34 promoter and the luciferase activity was examined using dual-luciferase reporter system. ***P<0.001 vs. oe-NC. (J) ChIP assay was used to verify the interaction between MNX1 and CCDC34 promoter. ***P<0.001 vs. anti-IgG. MNX1, Motor neuron and pancreas homeobox 1; CCDC34, coiled-coil domain-containing 34; LUAD, Lung adenocarcinoma; GEPIA, Gene Expression Profiling Interactive Analysis; sh, short hairpin RNA; oe, overexpression; NC, negative control (empty vector); RT-qPCR, Reverse transcription-quantitative PCR; ChIP, chromatin immunoprecipitation.

tumor growth in a LUAD animal model. The data suggested that an abnormally high level of MNX1 in tumor tissues may be a critical contributor to the poor prognosis of patients with LUAD and that MNX1 may serve as a potential candidate for therapeutic targets supporting the treatment of LUAD.

Transcription factors, a class of DNA-interacting proteins, have been reported to be involved in a wide spectrum of human diseases, such as cancer, in recent years. Of note,

transcription factors occupy ~20% of all identified oncogenes to date, becoming targets for cancer treatment (32). Coincidently, MNX1 encodes a homeobox transcription factor that promotes motor neuron differentiation and pancreatic development (33). In addition, MNX1 has been demonstrated to directly bind upstream of the TrkB gene to activate its expression, thereby suppressing adhesion and apoptosis of glioma cells and subsequently facilitating the
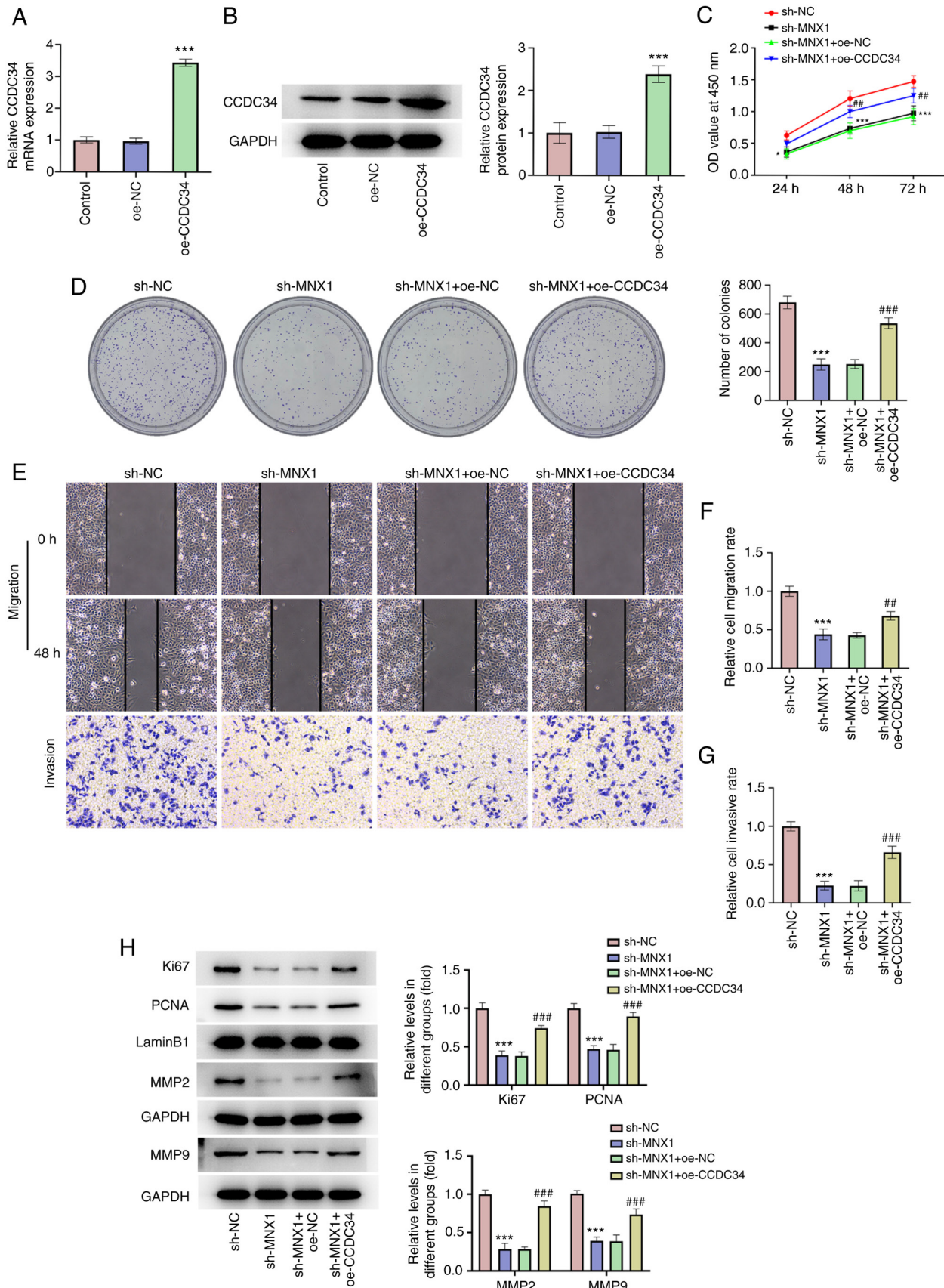
Figure 6. CCDC34 overexpression abolishes the inhibitory effect of MNX1 knockdown on proliferation, migration and invasion in A549 cells. Following transfection with oe-NC or oe-CCDC34 in A549 cells, (A) the mRNA level and (B) protein expression of CCDC34 were examined using reverse transcription-quantitative PCR and western blotting, respectively. $^{***}P<0.001$ vs. oe-NC. (C) CCK-8 assay was used to examine cell viability. (D) Cell colony formation assay was conducted to assay formed colonies. (E-G) Wound-healing and Transwell assays were performed to examine cell migration and invasion, respectively. Magnification, x100. (H) Protein expression of Ki67, PCNA, MMP2 and MMP9 was examined using western blot. $^{*}P<0.05$, $^{***}P<0.001$ vs. sh-NC. $^{##}P<0.01$, $^{###}P<0.001$ vs. sh-MNX1+oe-NC. CCDC34, coiled-coil domain-containing 34; MNX1, Motor neuron and pancreas homeobox 1; sh, short hairpin RNA; oe, overexpression; NC, negative control (empty vector); PCNA, proliferating cell nuclear antigen.
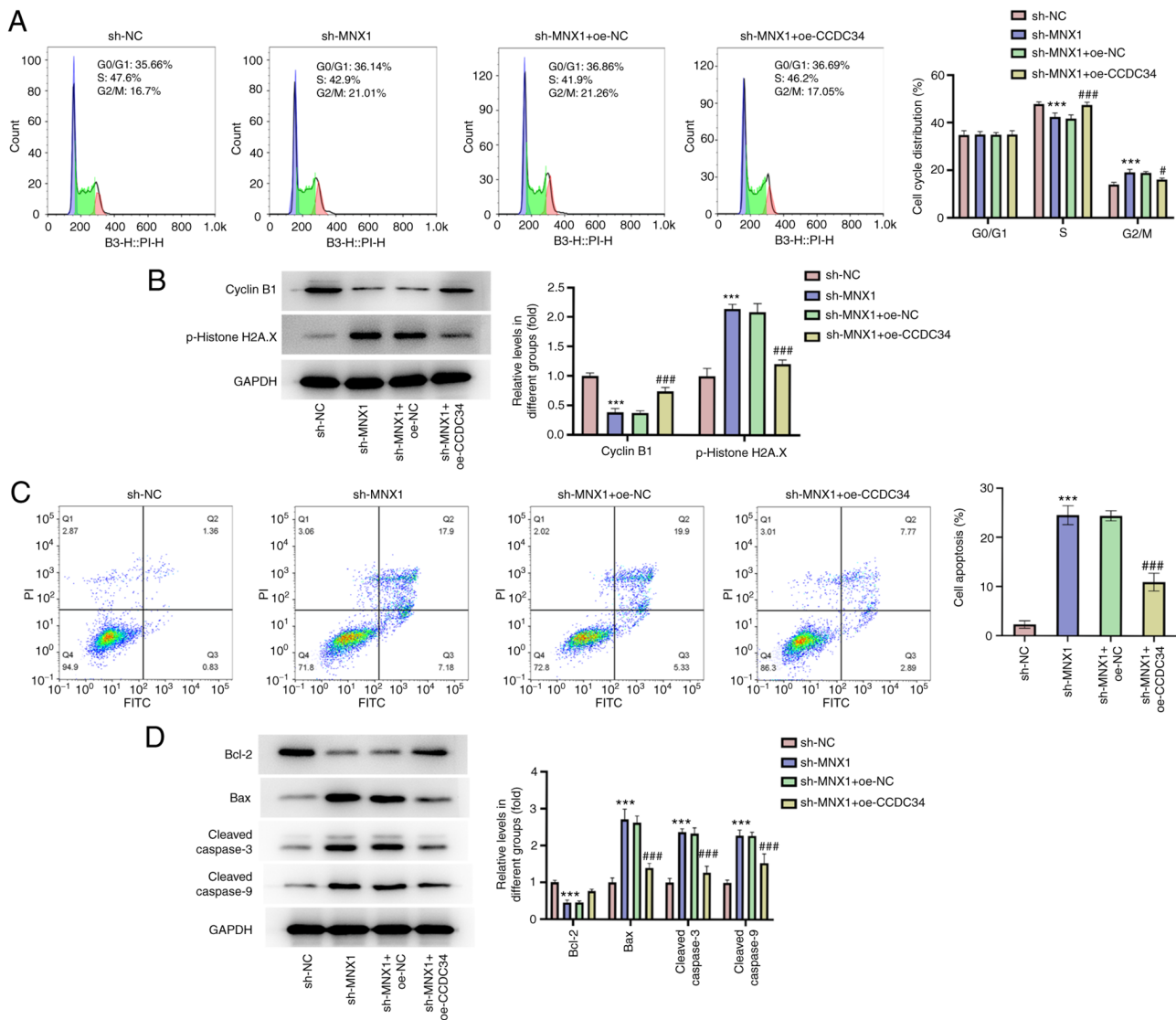
Figure 7. CCDC34 overexpression abolishes the function of MNX1 knockdown on cell cycle and apoptosis in A549 cells. (A) Cell cycle distribution was assessed using flow cytometry analysis. (B) Protein expression of cyclin B1 and p-Histone H2A.X was detected using western blotting. (C) Cell apoptosis rate was detected using flow cytometry analysis. (D) Protein expression of Bcl-2, Bax, cleaved-caspase3 and cleaved-caspase9 was detected using western blotting. ***P<0.001 vs. sh-NC; #P<0.05, ###P<0.001 vs. sh-MNX1+oe-NC. CCDC34, coiled-coil domain-containing 34; MNX1, Motor neuron and pancreas homeobox 1; sh, short hairpin RNA; oe, overexpression; NC, negative control (empty vector).

development of gliomas (34). In the present study, it was demonstrated that MNX1 may transcriptionally activate CCDC34 expression through binding to its promoter region. Previously published evidence revealed CCDC34 as a newly identified oncogene in several types of cancer. For instance, Geng *et al* (24) discovered an upregulated level of CCDC34 in colorectal cancer tissues compared with paracancerous tissues and CCDC34 silencing resulted in a decreased tumor invasion ability and an increase in cancer cell apoptosis. Gong *et al* (25) also uncovered the abnormal upregulation of CCDC34 in bladder cancer and demonstrated that the knockdown of CCDC34 may prevent bladder cancer cells from proliferating and migrating and may increase cell apoptosis and induce cell cycle arrest in G_2/M phase through inactivation of the MEK-ERK1/2-MAPK pathway. In the present study, it was revealed that the antineoplastic effect of MNX1 knockdown on the malignant phenotypes of LUAD cells *in vitro* were weakened following CCDC34 overexpression,

highlighting the critical role of the MNX1/CCDC34 axis during the progression of LUAD.

However, there are some limitations in the present study. Detection of clinical samples would be beneficial to validate the findings, which is now planned for future work. Meanwhile, the molecular mechanisms underlying MNX1/CCDC34 axis during the progression of LUAD still deserves to be further investigated.

In conclusion, to the best of the authors' knowledge, the present study demonstrated for the first time that MNX1 knockdown may repress the malignant phenotypes of LUAD cells *in vitro* and restrict tumor growth *in vivo*, revealing MNX1 as a potential oncogene in LUAD. In addition, the results identified that MNX1 may transcriptionally activate CCDC34 expression by binding directly to its promoter region. The antitumor activity of MNX1 knockdown was partly hindered by CCDC34 overexpression. Overall, the central theme of the findings of the present study provides evidence

of the association between the MNX1/CCDC34 axis and LUAD progression and provides novel insights of potential therapeutic targets for LUAD treatment.

Acknowledgements

Funding

Availability of data and materials

The datasets used and/or analyzed during the current study are available from the corresponding author on reasonable request.

Authors' contributions

WX designed the experiments; JW, CY, HL, JZ and LL obtained the data; JW, CY and HL analyzed and interpreted the data; JW and CY drafted the manuscript and WX revised the manuscript. JW and WX confirm the authenticity of all the raw data. All authors read and approved the final manuscript.

Ethics approval and consent to participate

All animal experiments were implemented in accordance with the guidelines and protocols for animal care and were approved by the Ethics Committee of Mianyang Central Hospital [approval no. S2021097 (01)].

Patient consent for publication

Not applicable.

Conflict of interest

The authors declare that they have no competing interests.

References

1. Sung H, Ferlay J, Siegel RL, Laversanne M, Soerjomataram I, Jemal A and Bray F: Global cancer statistics 2020: GLOBOCAN estimates of incidence and mortality worldwide for 36 cancers in 185 countries. CA Cancer J Clin 71: 209-249, 2021.
2. Ferlay J, Colombet M, Soerjomataram I, Parkin DM, Piñeros M, Znaor A and Bray F: Cancer statistics for the year 2020: An overview. Int J Cancer: Apr 5, 2021 (Epub ahead of print).
3. Sivakumar S, Lucas FAS, McDowell TL, Lang W, Xu L, Fujimoto J, Zhang J, Futreal PA, Fukuoka J, Yatabe Y, et al: Genomic landscape of atypical adenomatous hyperplasia reveals divergent modes to lung adenocarcinoma. Cancer Res 77: 6119-6130, 2017.
4. Xu F, He L, Zhan X, Chen J, Xu H, Huang X, Li Y, Zheng X, Lin L and Chen Y: DNA methylation-based lung adenocarcinoma subtypes can predict prognosis, recurrence, and immunotherapeutic implications. Aging (Albany NY) 12: 25275-25293, 2020.
5. Chen D, Wang R, Yu C, Cao F, Zhang X, Yan F, Chen L, Zhu H, Yu Z and Feng J: FOX-A1 contributes to acquisition of chemoresistance in human lung adenocarcinoma via transactivation of SOX5. EBioMedicine 44: 150-161, 2019.
6. Leotta CG, Federico C, Brundo MV, Tosi S and Saccone S: HLXB9 gene expression, and nuclear location during in vitro neuronal differentiation in the SK-N-BE neuroblastoma cell line. PLoS One 9: e105481, 2014.
7. Harrison KA, Druey KM, Deguchi Y, Tuscano JM and Kehrl JH: A novel human homeobox gene distantly related to proboscipedia is expressed in lymphoid and pancreatic tissues. J Biol Chem 269: 19968-19975, 1994.
8. Woolfe A, Goodson M, Goode DK, Snell P, McEwen GK, Vavouri T, Smith SF, North P, Callaway H, Kelly K, et al: Highly conserved non-coding sequences are associated with vertebrate development. PLoS Biol 3: e7, 2005.
9. Habener JF, Kemp DM and Thomas MK: Minireview: Transcriptional regulation in pancreatic development. Endocrinology 146: 1025-1034, 2005.
10. Vult von Steyern F, Martinov V, Rabben I, Nja A, de Lapeyriere O and Lomo T: The homeodomain transcription factors Islet 1 and HB9 are expressed in adult alpha and gamma motoneurons identified by selective retrograde tracing. Eur J Neurosci 11: 2093-2102, 1999.
11. Bonnefond A, Vaillant E, Philippe J, Skrobek B, Lobbens S, Yengo L, Huyvaert M, Cavé H, Busiah K, Scharfmann R, et al: Transcription factor gene MNX1 is a novel cause of permanent neonatal diabetes in a consanguineous family. Diabetes Metab 39: 276-280, 2013.
12. Chen H, Zeng L, Zheng W, Li X and Lin B: Increased expression of microRNA-141-3p improves necrotizing enterocolitis of neonates through targeting MNX1. Front Pediatr 8: 385, 2020.
13. Merello E, De Marco P, Ravegnani M, Riccipetitoni G, Cama A and Capra V: Novel MNX1 mutations and clinical analysis of familial and sporadic Currarino cases. Eur J Med Genet 56: 648-654, 2013.
14. Das M: MNX1: A novel prostate cancer oncogene. Lancet Oncol 17: e521, 2016.
15. Zhu B, Wu Y, Luo J, Zhang Q, Huang J, Li Q, Xu L, Lu E and Ren B: MNX1 promotes malignant progression of cervical cancer via repressing the transcription of p21^{cip1}. Front Oncol 10: 1307, 2020.
16. Yang X, Pan Q, Lu Y, Jiang X, Zhang S and Wu J: MNX1 promotes cell proliferation and activates Wnt/β-catenin signaling in colorectal cancer. Cell Biol Int 43: 402-408, 2019.
17. Tian T, Wang M, Zhu Y, Zhu W, Yang T, Li H, Lin S, Dai C, Deng Y, Song D, et al: Expression, clinical significance, and functional prediction of MNX1 in breast cancer. Mol Ther Nucleic Acids 13: 399-406, 2018.
18. McFarlane AA, Orriss GL and Stetefeld J: The use of coiled-coil proteins in drug delivery systems. Eur J Pharmacol 625: 101-107, 2009.
19. Wang J, Wu X, Dai W, Li J, Xiang L, Tang W, Lin J, Zhang W, Liu G, Yang Q, et al: The CCDC43-ADRM1 axis regulated by YY1, promotes proliferation and metastasis of gastric cancer. Cancer Lett 482: 90-101, 2020.
20. Bai L, Yang ZX, Liu JS, Wang DS and Yu HC: Prognostic significance of CCDC137 expression and its association with immune infiltration in hepatocellular carcinoma. Dis Markers 2022: 5638675, 2022.
21. Zhang X, Zheng Q, Wang C, Zhou H, Jiang G, Miao Y, Zhang Y, Liu Y, Li Q, Qiu X and Wang E: CCDC106 promotes non-small cell lung cancer cell proliferation. Oncotarget 8: 26662-26670, 2017.
22. Kutsche K, Glauner E, Knauf S, Pomarino A, Schmidt M, Schröder B, Nothwang H, Schüler H, Goecke T, Kersten A, et al: Cloning and characterization of the breakpoint regions of a chromosome 11;18 translocation in a patient with hamartoma of the retinal pigment epithelium. Cytogenet Cell Genet 91: 141-147, 2000.
23. Lin Z, Qu S, Peng W, Yang P, Zhang R, Zhang P, Guo D, Du J, Wu W, Tao K and Wang J: Up-Regulated CCDC34 contributes to the proliferation and metastasis of hepatocellular carcinoma. Onco Targets Ther 13: 51-60, 2020.
24. Geng W, Liang W, Fan Y, Ye Z and Zhang L: Overexpression of CCDC34 in colorectal cancer and its involvement in tumor growth, apoptosis and invasion. Mol Med Rep 17: 465-473, 2018.
25. Gong Y, Qiu W, Ning X, Yang X, Liu L, Wang Z, Lin J, Li X and Guo Y: CCDC34 is up-regulated in bladder cancer and regulates bladder cancer cell proliferation, apoptosis and migration. Oncotarget 6: 25856-25867, 2015.

26. Livak KJ and Schmittgen TD: Analysis of relative gene expression data using real-time quantitative PCR and the 2(-Delta Delta C(T)) Method. Methods 25: 402-408, 2001.
27. Giglia-Mari G, Zotter A and Vermeulen W: DNA damage response. Cold Spring Harb Perspect Biol 3: a000745, 2011.
28. Shi J, Hua X, Zhu B, Ravichandran S, Wang M, Nguyen C, Brodie SA, Palleschi A, Alloisio M, Pariscenti G, *et al*: Somatic genomics and clinical features of lung adenocarcinoma: A retrospective study. PLoS Med 13: e1002162, 2016.
29. Siegel RL, Miller KD and Jemal A: Cancer statistics, 2018. CA Cancer J Clin 68: 7-30, 2018.
30. Su L, Zhao J, Su H, Wang Y, Huang W, Jiang X and Gao S: CircRNAs in lung adenocarcinoma: Diagnosis and therapy. Curr Gene Ther 22: 15-22, 2022.
31. Chen M, Wu R, Li G, Liu C, Tan L, Xiao K, Ye Y and Qin Z: Motor neuron and pancreas homeobox 1/HLXB9 promotes sustained proliferation in bladder cancer by upregulating CCNE1/2. J Exp Clin Cancer Res 37: 154, 2018.
32. Lambert M, Jambon S, Depauw S and David-Cordonnier MH: Targeting transcription factors for cancer treatment. Molecules 23: 1479, 2018.
33. Harrison KA, Thaler J, Pfaff SL, Gu H and Kehrl JH: Pancreas dorsal lobe agenesis and abnormal islets of Langerhans in Hlxb9-deficient mice. Nat Genet 23: 71-75, 1999.
34. Jiang L, Chen S, Zhao D, Yan J, Chen J, Yang C and Zheng G: MNX1 reduces sensitivity to anoikis by activating TrkB in human glioma cells. Mol Med Rep 18: 3271-3279, 2018.